lubricants

MDPI

Article

Tribological and Micro-Mechanical Behaviors of Advanced Polyethylene (HDPE) by Radiation

Martin Ovsik *, Adam Cesnek, Adam Pis, Klara Fucikova and Michal Stanek

Faculty of Technology, Tomas Bata University in Zlin, Vavreckova 5669, 760 01 Zlin, Czech Republic; a_cesnek@utb.cz (A.C.); a_pis@utb.cz (A.P.); k_fucikova@utb.cz (K.F.); stanek@utb.cz (M.S.)
* Correspondence: ovsik@utb.cz

Abstract

This study examines the tribological and micro-mechanical behavior of high-density polyethylene (HDPE), which has been advanced to the class of advanced polymers through electron beam irradiation (irradiation dose of 33 kGy to 198 kGy). The tribological and mechanical behaviors were analyzed at the surface and at various depths beneath the surface to verify the extent of radiation effects across the entire cross-section of the specimen. Changes in tribological and mechanical behavior are closely related to changes in the structure of the material, mainly changes in crystallinity. As this study shows, 99 kGy appears to be the ideal radiation dose in terms of the properties examined. An increase in absorbed radiation dose leads to a deterioration of tribological and mechanical performance, which correlates with material degradation and a concomitant reduction in crystallinity. The improvement in the properties examined between unirradiated and irradiated HDPE at a dose of 99 kGy is 18% for mechanical behaviors and 8% for tribological behaviors on the surface of the sample. A maximum deviation of 39% was identified between the surface and the center of the material. There was also a change in crystallinity of up to 12%. These modifications result in enhanced surface wear resistance and increased overall stiffness, effectively shifting commodity-grade HDPE toward the performance domain of advanced polymers with only minimal cost implications.

Keywords: electron irradiation; polyethylene; extent of crosslinking; crystalline content; tribological behavior; instrumented indentation hardness; coefficient of friction

1. Introduction

The micro-mechanical behaviors of irradiated polyethylene have been a subject of significant research interest, with studies focusing on the effects of various types of irradiation on the mechanical, tribological and morphological characteristics of polyethylene. By examining the changes induced by irradiation at the nano and micro levels, researchers can gain a comprehensive understanding of how irradiation influences the performance of polyethylene materials. These insights are crucial for optimizing the design and utilization of irradiated polyethylene in various engineering and industrial applications.

The cross-linking of polymer materials was first studied in detail in the case of polyethylene, which primarily exhibits a cross-linking reaction when exposed to ionizing radiation. This is due to the fact that polyethylene has a relatively free main chain [1].

The first descriptions of chemical changes in polyethylene produced by radiation were reported by Dolem (30). The work described the change in weight of polyethylene films

Received: 21 January 2026
Revised: 6 February 2026
Accepted: 9 February 2026
Published: 12 February 2026

irradiated in a vacuum due to the release of hydrogen and low-molecular-weight hydrocarbons. A detailed study of the effect of radiation on polyethylene was then conducted by Charlesby in 1952. The author convincingly demonstrated that polyethylene cross-links after exposure to ionizing radiation [2].

The advantage of radiation crosslinking of thermoplastics using ionizing radiation, especially β (electron) radiation, is the high speed of delivery of the required radiation dose (seconds). Crosslinking of thermoplastics takes place at room temperature in air, which can be considered energy-efficient compared to chemical methods, where heat must be supplied for the crosslinking reaction to take place. However, the action of ionizing radiation causes the polymer material to heat up by 0.43–0.95 °C/kGy, and therefore a suitable radiation dose must be selected to prevent damage to the original material due to excessive heating. If necessary, multiple irradiations at lower doses are selected to ensure the desired properties of the final product. Another advantage over chemical modification methods is the reduction in the content of volatile organic compounds and toxic chemicals required to achieve a cross-linking reaction using peroxide and silane. The radiation cross-linking process is not dependent on ambient humidity, eliminating the need for special packaging in vacuum bags, which ensures constant conditions without the presence of moisture, which is very important in the silane cross-linking process to prevent premature cross-linking [3–5]. The papers listed below only cover the issue in a limited way, or just certain aspects of it, and do not focus on a comprehensive description of how radiation affects the properties of polyethylene. The term "cross-linked polymers" refers to chains of macromolecular substances whose macromolecules are interconnected by chemical bonds to form a three-dimensional spatial network. They are formed either by cross-linking a linear or branched polymer, or by the mutual reaction of two or more monomers with a formal functionality (i.e., the ability to form a chemical bond) greater than 2.

When exposed to ionizing radiation, polyethylene primarily exhibits a cross-linking reaction. This is due to the fact that polyethylene has a relatively free main chain. The formation of cross-links occurs mainly in the amorphous regions of polyethylene, with the ratio between cross-linking in amorphous regions and in crystalline regions reaching a value of 3.6. Macromolecules in the amorphous regions of the polymer are intertwined, which predestines them for cross-linking. In the crystalline regions of the polymer, the free radicals formed are localized near the surface of the crystallites, and thus the cross-links formed are located at their edges. In the case of polyethylene, the resulting cross-links are therefore formed mainly in the amorphous region, but localized to the surface of the crystallites.

Collectively, these studies indicate that irradiation can modify local stiffness, hardness, and deformation mechanisms in PE by promoting crosslinking and structural changes within the surface or near-surface region, thereby altering micro-mechanical responses at small scales relevant to indentation and surface deformation [6–8].

In multimethod evaluations, comparisons between non-crosslinked, moderately crosslinked, and highly crosslinked polyethylene's show a significant reduction in wear in wear tests simulated in the knee or hip joint area with a higher degree of crosslinking, which is consistent with the idea that micro-hardening translates into improved resistance to material removal during sliding wear, although the transition from micro-indentation to macro wear is mediated by tribological kinematics and debris formation [9,10].

Radiation-induced crosslinking increases stiffness and can reduce toughness in amorphous regions, thereby affecting crack initiation and propagation near stress concentrators such as cracks or defects. Elevated irradiation doses can modify fatigue-crack growth resistance and fracture toughness, with some studies noting increased resistance to crack

initiation for certain crosslinked grades, while others observe embrittlement in highly crosslinked networks [11,12].

For effective linking of micro-mechanical behaviors with the underlying microstructure, micro-mechanical measurements must be integrated with nanoscale and mesoscale structural characterizations (e.g., crystallinity, lamellar spacing, free volume metrics); this integrated approach supports predictive modeling of irradiated PE performance in real-world applications [8,13,14]. Electron beam and gamma irradiation have been shown to affect crystallinity and mechanical behaviors in various polyethylenes, with nuances depending on environment and dose. In many cases, irradiation increases yield strength and modulus but may reduce elongation at break or toughness if followed by unfavorable post-irradiation treatments [15,16]. Higher irradiation doses generally increase crosslink density, which can reduce wear but may decrease ductility and fracture toughness due to embrittling effects in amorphous regions. Experimental work suggests that irradiation dose affects modulus, yield, and crystallinity, with increasing doses sometimes leading to an initial rise in stiffness followed by degradation depending on environmental conditions and post-treatment, particularly when oxidation is allowed to proceed [17].

Radiation can predominantly induce crosslinking in PE, notably within the amorphous regions, enhancing network integrity and potentially increasing surface hardness and modulus in irradiated surface layers, especially at elevated doses where crosslink density is heightened. Conversely, chain scission and oxidative processes may degrade crystalline regions, leading to embrittlement; the extent of these effects varies based on polymer type, dose, and environmental conditions, with macroscopic wear and fracture behaviors reflecting the interplay of these pathways [18–20].

Oxidative degradation linked with irradiation impacts free radical chemistry and long-term stability, affecting micromechanical behavior in retrieved or aged components. Models exploring three-phase systems and oxidation-induced transformations have been utilized to explain micromechanical trends in irradiated PE and related ultra-high molecular weight variants [13,14,18].

Radiation-induced crosslinking is known to enhance the mechanical and tribological performance of polymeric materials while simultaneously improving their resistance to thermal and chemical loading. Owing to these property gains, such materials are commonly employed across a broad range of industrial sectors, including automotive and electromobility applications, electrical and mechanical engineering, construction, and medical technologies. Representative uses encompass fuel, pressure, and suction lines, heat-shrinkable products, sealing elements, electrical insulation for cables and conductors, as well as tubing for medical devices.

Compared to previous studies, we intended to systematically study the effect of electron radiation across the entire thickness of the sample and focus on individual layers beneath the surface. The present study focuses on quantifying the influence of electron irradiation on the tribological and micromechanical response of polymers, with particular attention given to high-density polyethylene. Material characterization was performed using depth-sensing indentation, a technique with sufficient sensitivity to capture irradiation-induced structural modifications, especially variations in crystallinity that directly affect mechanical and tribological behaviors. Unlike most existing studies, which primarily report surface-level effects, this work systematically examines property changes across the full specimen thickness, including both the surface layer and subsurface regions at increasing depths. To the authors' knowledge, a comprehensive assessment of radiation effects throughout the entire cross-section of HDPE has not yet been reported in the available literature.

2. Materials and Methods

The presented study describes the effect of electron radiation on the tribological and micro-mechanical behaviors of high-density polyethylene. The results were supplemented by measuring the cross-linking content and crystallinity using wide-angle X-ray diffraction, which indicates changes in structure due to radiation. Each parameter was determined from ten repeated measurements, with the results evaluated using the arithmetic mean and standard deviation. The connecting lines between individual measurements do not express linear behavior, but only highlight the trend.

2.1. Material

High-density polyethylene (HDPE) with the designation HDPE DOW 25055E from Dow Chemical Company (Midland, MI, USA) was selected as the test material. Polyethylene was chosen because radiation cross-linking does not require the addition of multifunctional monomers (cross-linking agents) to the structure (polymer matrix), which are added to polymer materials mainly to improve the efficiency of the cross-linking process.

High-density polyethylene was selected due to its broad applicability in engineering practice. When modified by electron irradiation, its performance characteristics can be shifted from those typical of commodity polymers toward levels commonly associated with higher-cost technical materials. The radiation-induced structural modifications contribute to enhanced mechanical and tribological performance, thereby extending the practical application range of HDPE.

2.2. Manufacture of Injection-Molded Specimens

Test specimens in the form of tensile bars measuring 10 × 4 × 80 mm (according to ČSN EN ISO 527-2) [21] were produced on an ARBURG ALLROUNDER 470 E 1000—290 injection molding machine from Arburg (Losburg, Germany). A Regloplas 150 intelligent oil temperature control unit from Regoplast (Gallen, Switzerland) was used to control the mold temperature.

Injection molding parameters for high-density polyethylene (HDPE) were chosen based on the manufacturer's specifications and practical experience with the machine, ensuring that the resulting test specimens were optimized for dimensional accuracy and geometric consistency. The selected injection parameters are listed in Table 1.

Table 1. Technological parameters of HDPE injection molding.

Technological Parameter	Unit	Value
Injection pressure	MPa	80
Injection speed	mm/s	60
Length of a dose	mm	40
Temperature under the hopper	°C	60
Cooling time	s	20
Holding pressure	MPa	60
Holding pressure duration	s	25
Mold temperature	°C	40
Heat zones settings		
Zone n. 1	°C	200
Zone n. 2	°C	205
Zone n. 3	°C	210
Zone n. 4	°C	225

2.3. Electron Beam Irradiated

The irradiation of test specimens was carried out in Germany in cooperation with BGS Beta-Gamma Service (Wiehl, Germany). The source of electron beta radiation was

a high-voltage Rhodotron accelerator with a maximum energy of 10 MeV. High-density polyethylene does not require the addition of a cross-linking agent for the cross-linking process and was therefore irradiated with commercially available polyethylene. The radiation doses were 33, 66, 99, 132, 165, and 198 kGy. One pass under the scanning device meant that the test specimens were irradiated with a dose of 33 kGy. Irradiation to the required dose is therefore based on successive passes of the test specimens under the scanning device in order to reduce the thermal load on the test specimens.

2.4. Surface Quality

The surface quality of the individual test samples was measured using a non-contact optical device, the Keyence VK-X300 from Keyence (Osaka, Japan). The parameters used for measurement are listed in Table 2. The arithmetic mean deviation Ra was selected as the evaluated parameter. All parameters were measured in 10 sections and then statistically evaluated.

Table 2. Surface quality measurement parameters.

Surface Quality Parameters	Unit	Value
Area of measurement L × W	mm	1 × 1.5
Measurement length	mm	1.3

2.5. Micro-Tribology Behaviors

Tribological behaviors were analyzed using the MicroCombi Tester MCT^3 by Anton Paar (Graz, Austria). A micro-abrasion test was performed to assess both the coefficient of friction and the abrasion resistance of the tested surfaces. The concept consisted of pressing a diamond cone (Rockwell type, apex angle 120°, tip radius 100 µm) into the surface of the sample, with the indenter performing a linear motion under constant load. The tribological behaviors were assessed at three distinct load levels of 0.5 N, 1 N, and 5 N, which made it possible to evaluate the effect of different measurement depths on the measured values. The test parameters are shown in Table 3. The load values were selected based on the technical capabilities of the equipment and findings from previous research.

Table 3. Configuration of tribological test conditions.

	Tribological Parameter		
Measurement load (N)	0.5	1	5
Speed (mm/min)	10	10	10
Measurement length (mm)	5	5	5
Acquisition Rate (Hz)	30	30	30

The indentation process was conducted in the following manner: before the indenter engaged the material, a sensing force was applied along the surface to calibrate and initialize the measurement system. When the normal force Fn was applied, the indenter penetrated the test sample, causing deformation of the material and creating an indentation. The measurement system recorded the friction force Ft, which is directly proportional to the applied normal load, along with the surface profile of the sample, both before indentation (Pd, initial depth) and after indentation (Rd, residual depth resulting from polymer relaxation). The difference between Pd and Rd provided insights into the elastic and viscoelastic behavior of polyethylene. Critical loads were determined with precision using acoustic emission (AE) analysis in combination with the coefficient of friction µ.

The Scratch test method was used to measure tribological properties, which serves to determine the surface resistance of thin polymer layers against scratching. In addition to

the scratch test, other methods such as the pin-on-disk or four-ball test could also be used to measure tribological properties. The choice between the scratch test and the pin-on-disk or four-ball test depended on whether the plan was to examine surface resistance or long-term wear processes. Many polymer products (car dashboards, displays, consumer electronics) fail due to aesthetic damage (scratches) rather than overall material wear. The advantage of the Scratch test over other methods is that it accurately simulates a single penetration by a hard object (e.g., a key or fingernail) and allows the study of failure mechanisms such as crack formation, fish-scale patterns, or polymer whitening (crazing).

2.6. Micro-Mechanical Behaviors

Micro-mechanical behaviors were assessed using the MicroCombi Tester MCT^3 by Anton Paar (Graz, Austria). Evaluation was carried out using the Depth Sensing Indentation (DSI) method according to EN ISO 14577 [22–25]. According to this standard, the following mechanical parameters were evaluated: indentation hardness (H_{IT}), indentation modulus (E_{IT}), indentation creep (C_{IT}), and indentation depth (h_{max}), which were analyzed using the Oliver–Pharr method. A four-sided diamond cone (Vickers) with a tip angle of 136° was used as the measuring tip. The measurements were performed at the same loads (0.5 N, 1 N, and 5 N) as for the tribological characteristics in order to capture changes not only on the surface of the sample but also in the lower layers. The measurement parameters are shown in Table 4.

Table 4. Configuration of micro-indentation test conditions.

Indentation Parameters			
Indentation load (N)	0.5	1	5
Load endurance time (s)	90	90	90
Loading/de-loading speed (m/s)	1	2	10

Micro-mechanical behaviors were measured not only in the surface layers under loads of 0.5 N, 1 N, and 5 N, but also at different depths within the material, where a load of 0.5 N was selected.

To enable measurements at different depths, the irradiated specimens were sectioned and subsequently polished.

A Buehler (Leinfelden-Echterdingen, Germany) IsoMet 4000 precision laboratory saw equipped with a diamond grinding wheel was employed for cutting the samples into individual segments. To minimize thermal effects during sectioning, the cutting zone was cooled using a cooling fluid. The rotation speed of the wheel was set to 1800 rpm.

The individual cut segments were cast in resin in a 40 mm diameter mold and then cured. The resin used in this process was marketed under the trade name EpoxiCure and was supplied by Buehler.

An EcoMet 250 Pro machine with an AutoMet 250 rotary head, also manufactured by Buehler, was employed to grind the individual layers and subsequently polish the segments. The following parameters were set on the machine: head speed at 40 rpm, table speed at 100 rpm, and sample clamping force at 20 N. To ensure sufficient cooling and chip removal, water was continuously supplied to the grinding site. Grinding was carried out in several steps, using grinding wheels with progressively finer grit sizes (P180, P320, P600, and P1200). Polishing of the samples was carried out using diamond suspensions with particle sizes of 9 µm and 3 µm. The polishing process was subsequently performed without active cooling.

The basic and most important parameter evaluated was the H_{IT} indentation hardness, defined as a measure of resistance to permanent deformation or surface damage.

Indentation hardness is determined from the peak load force F_{MAX} and the contact area between the indenter and the test specimen A_P. The indentation area A_p is determined from the geometry of the indenter and the contact depth h_c, which is less than the total depth because it takes into account the elastic deformation of the material at the edge of the indentation [22–27].

$$H_{IT} = \frac{F_{max}}{A_p} \tag{1}$$

$$A_p = 23.96 \cdot h_c^2 \tag{2}$$

Another important mechanical property is the indentation modulus, which characterizes the stiffness of the measured HDPE. Using the Oliver Pharr method, the indentation modulus E_{IT} is calculated from the reduced modulus E_r and the complex modulus E^*. The indentation modulus is determined from the tangent of the relaxation curve. Where E_r is the reduced modulus, E_i is the modulus of elasticity of the indenter, ν_i is the Poisson's ratio of the indenter, and ν_s is the Poisson's ratio of the measured body (0.4 is selected for HDPE). The reduced modulus is determined from the projection of the contact area A_p and the contact compliance C.

Ideally, the indentation modulus corresponds to the modulus of elasticity (Young's modulus) [22–27].

$$E_{IT} = E^* \cdot \left(1 - \mathrm{v}_s^2\right) \tag{3}$$

$$E^* = \frac{1}{\frac{1}{E_r} - \frac{1-v_i^2}{E_i}} \tag{4}$$

$$E_r = \frac{\sqrt{\pi}}{2 \cdot C\sqrt{A_p}} \tag{5}$$

Indentation creep (C_{IT}) is calculated from the change in penetration depth under a constant load, where h_1 represents the indentation depth at time t_1, when the test load is applied, and h_2 is the depth at time t_2 during the hold at the maximum load [22–27].

$$C_{IT} = \frac{h_2 - h_1}{h_1} 100 \tag{6}$$

2.7. Structural Behaviors

Electron radiation has a significant effect on structural changes (crystallinity), which subsequently manifest themselves in changes in tribological and micro-mechanical behaviors. These structural changes were investigated using gel testing and wide-angle X-ray diffraction.

2.7.1. Gel Test

To assess the degree of crosslinking, a gel content test was conducted in accordance with EN ISO 579 [28]. In this case, 1 g of solid sample cut from the whole modified HDPE sample was weighed and mixed with 200 mL of solvent, i.e., xylene. The mixture was boiled for 8 h at a temperature of 140 °C while stirring intensively. The solvent dissolved the amorphous part of the tested HDPE, while the cross-linked part remained undissolved. The gel and the dissolved phase were then separated. After separation, the gel was dried for 8 h in a vacuum at 100 °C. The dried residue was weighed again. The mass of the dried residue is measured and related to the initial bulk mass, and the degree of crosslinking is calculated as a percentage.

2.7.2. Wide-Angle X-Ray Diffraction

Wide-angle X-ray diffraction was conducted to characterize the crystalline structure at both the sample surface and the cross-sectional center. The measurements were carried out on an X'PERT PRO MPD diffractometer (PANalytical, Malvern, UK) under operating conditions of 40 kV and 30 mA. Diffraction data were collected over a 2θ range of 10–30° with a step size of 0.013°, employing CuKα radiation with a nickel filter. Crystallinity (X_c) was calculated as the ratio of the crystalline peak area (A_c) to the amorphous area (A_a) after background correction.

$$X_C = \frac{A_c}{A_a + A_c} 100 \quad (7)$$

3. Results

This study focuses on the comprehensive characterization of the tribological and micro-mechanical behaviors of high-density polyethylene (HDPE) modified by electron beam irradiation. Tribological behaviors such as frictional force, acoustic emission, friction coefficient, and removal depth were examined, as well as micro-mechanical behaviors such as indentation hardness, indentation modulus, and indentation creep. Changes in the examined properties are caused by changes in the morphology (structure) of HDPE due to electron irradiation. These morphological properties include the degree of cross-linking and the volume of the crystalline phase. To evaluate the impact of electron irradiation across the entire thickness of the tested sample, all investigated properties were determined not only in the surface layer but also at various depths below the sample surface. The main emphasis is placed on the characterization of tribological and micro-mechanical behaviors together with structural behaviors (degree of cross-linking and crystallinity volume) of HDPE irradiated with electron radiation across the entire cross-section of the sample.

3.1. Surface Quality

Surface quality (Figure 1, Table A1) was measured to assess the effect of electron radiation on changes in surface topography that could influence the measured tribological and micro-mechanical properties. As shown by the results of surface quality measurements of the tested HDPE, electron radiation has no statistically significant effect on surface quality changes. The surface quality Ra of the unirradiated original HDPE was measured at 0.66 µm, and the surface quality Ra of the HDPE irradiated with a dose of 99 kGy was measured at 0.61 µm. For all other radiation doses, the surface quality Ra was measured at similar values. It can therefore be concluded that electron radiation does not affect surface quality and, consequently, tribological and micro-mechanical properties are not affected.

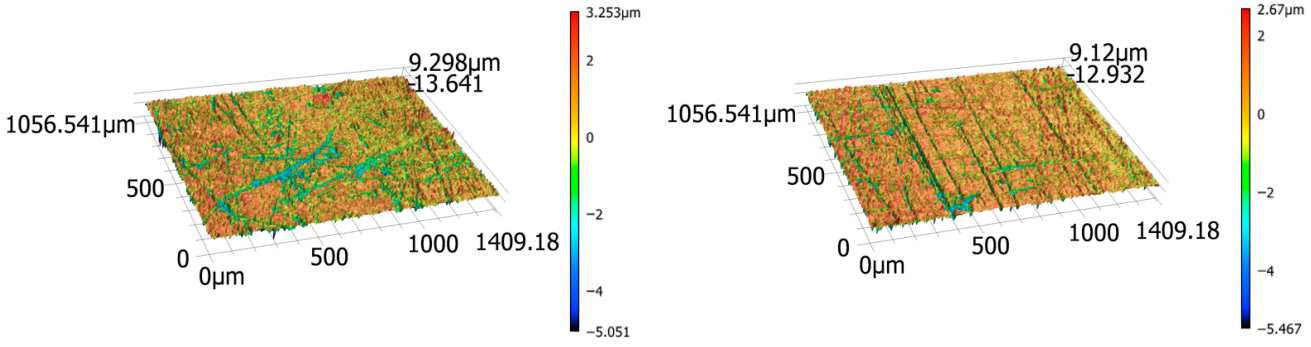

(**a**) (**b**)

Figure 1. *Cont.*

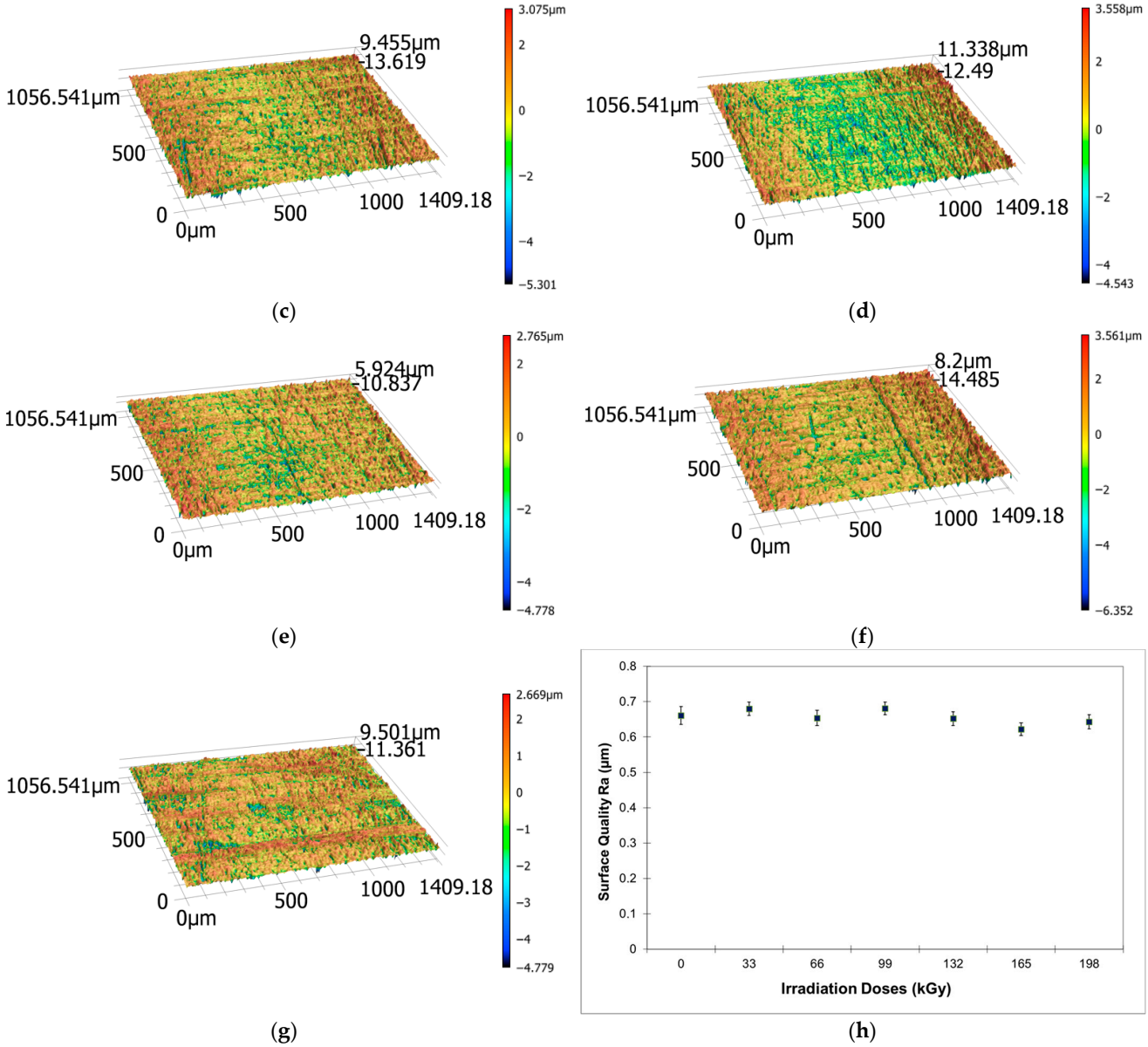

Figure 1. Surface quality: (**a**) 0 kGy; (**b**) 33 kGy; (**c**) 66 kGy; (**d**) 99 kGy; (**e**) 132 kGy; (**f**) 165 kGy; (**g**) 198 kGy; (**h**) surface quality Ra.

3.2. Micro-Tribological Behaviors—Scratch Test

A scratch tester was employed to evaluate the friction and wear behavior of the layers, measuring friction force, acoustic emission, coefficient of friction, and depth at three load forces of 0.5 N, 1 N, and 5 N. The tribological behavior of HDPE shows the surface's resistance to mechanical damage due to friction. Irradiation increases the resistance of the surface. For clarity, Figures 2–4 show only the curves for unirradiated HDPE and HDPE irradiated with a dose of 99 kGy.

It should also be noted that tribological interaction with the counterface material is fundamental to the concept of a tribosystem and plays a key role in interpreting results and actual system wear. In this measurement, the tested material was HDPE polymer and the counterface was a diamond cone (Rockwell) indenter. The tribological compatibility of the diamond cone-HDPE polymer combination utilizes the ability of plastic to absorb hard abrasive particles into its structure, thereby protecting the opposing diamond cone from wear. This phenomenon is called dry lubrication with high resistance to seizing, as stated by

the authors in their works [29–31]. During operation, a thin layer of polymer is transferred to the metal surface. Friction then does not occur in the "plastic-metal" mode, but more effectively as "plastic-plastic," which dramatically reduces wear, and it can be stated that the wear of the diamond cone in this case is negligible. Table 5 and Figure 2 show the results of the tribological behaviors of irradiated HDPE at an applied load of 0.5 N. For all tribological behaviors, friction force (Figure 2a), acoustic emission (Figure 2b), coefficient of friction (Figure 2c), and depth of wear (Figure 2d), an improvement in properties due to irradiation of HDPE was measured. For instance, the coefficient of friction of non-irradiated HDPE was 0.28, while irradiation at 99 kGy reduced it to 0.26. The improvement in the coefficient of friction resulting from radiation was 8%. Higher radiation doses did not lead to an increase in tribological behaviors, but rather to a slight deterioration due to the onset of material degradation caused by radiation.

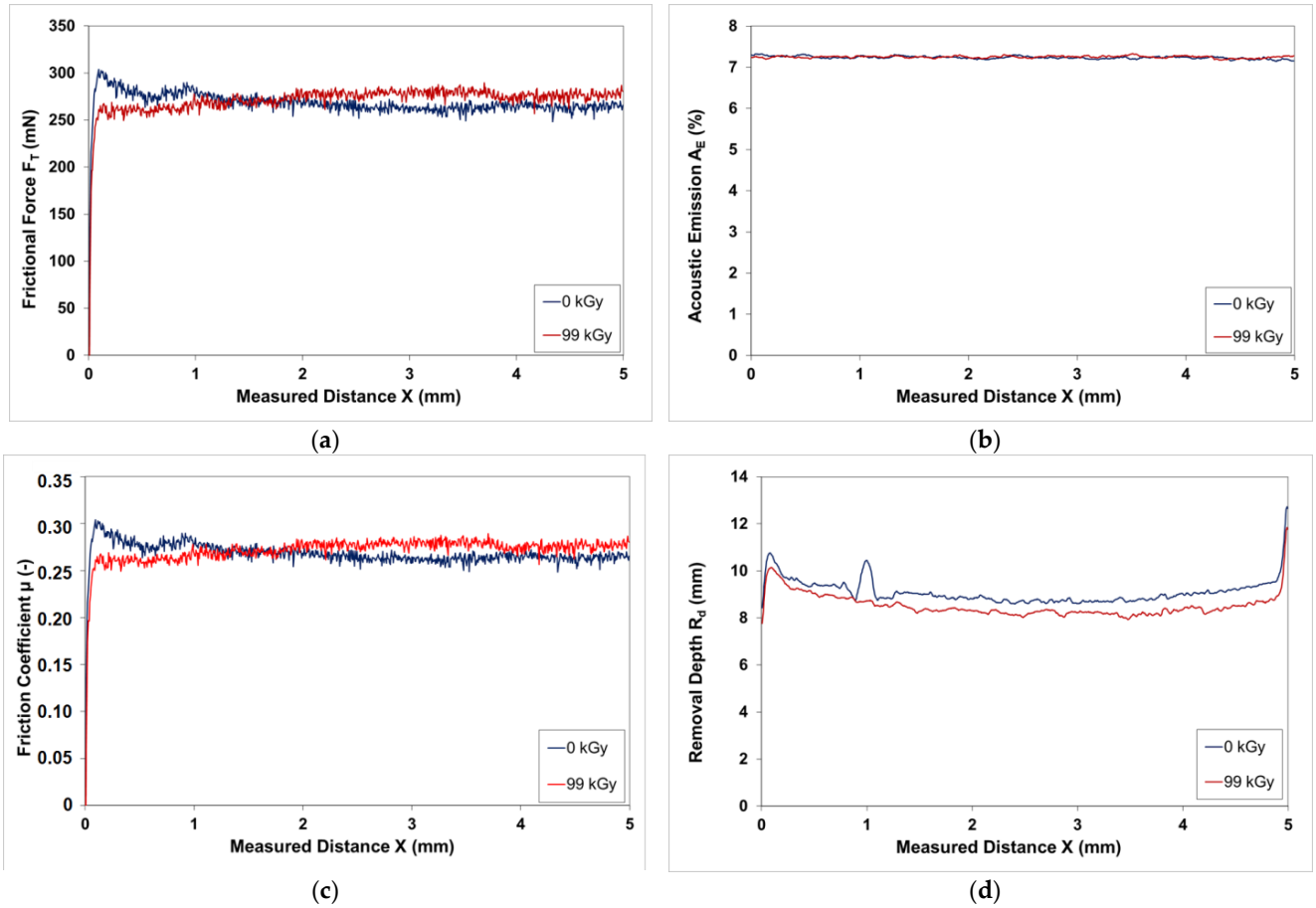

Figure 2. Tribological behaviors at a load of 0.5 N: (**a**) Frictional force; (**b**) Acoustic emission; (**c**) Friction coefficient; (**d**) Removal depth.

The tribological behaviors of irradiated HDPE are shown in Table 6 and Figure 3. All monitored tribological behaviors (friction force, acoustic emission, friction coefficient, and layer removal) improved due to the effect of electron radiation on HDPE. Non-irradiated HDPE showed the highest values; however, the tribological behaviors improved due to radiation at a dose of 99 kGy. For example, the friction coefficient measured for non-irradiated HDPE was 0.32, while for irradiated HDPE with a dose of 99 kGy, the friction coefficient measured was 0.3. Radiation treatment caused a 7% improvement in the friction coefficient. Increasing radiation dose caused a deterioration in tribological behaviors due to the onset of degradation processes.

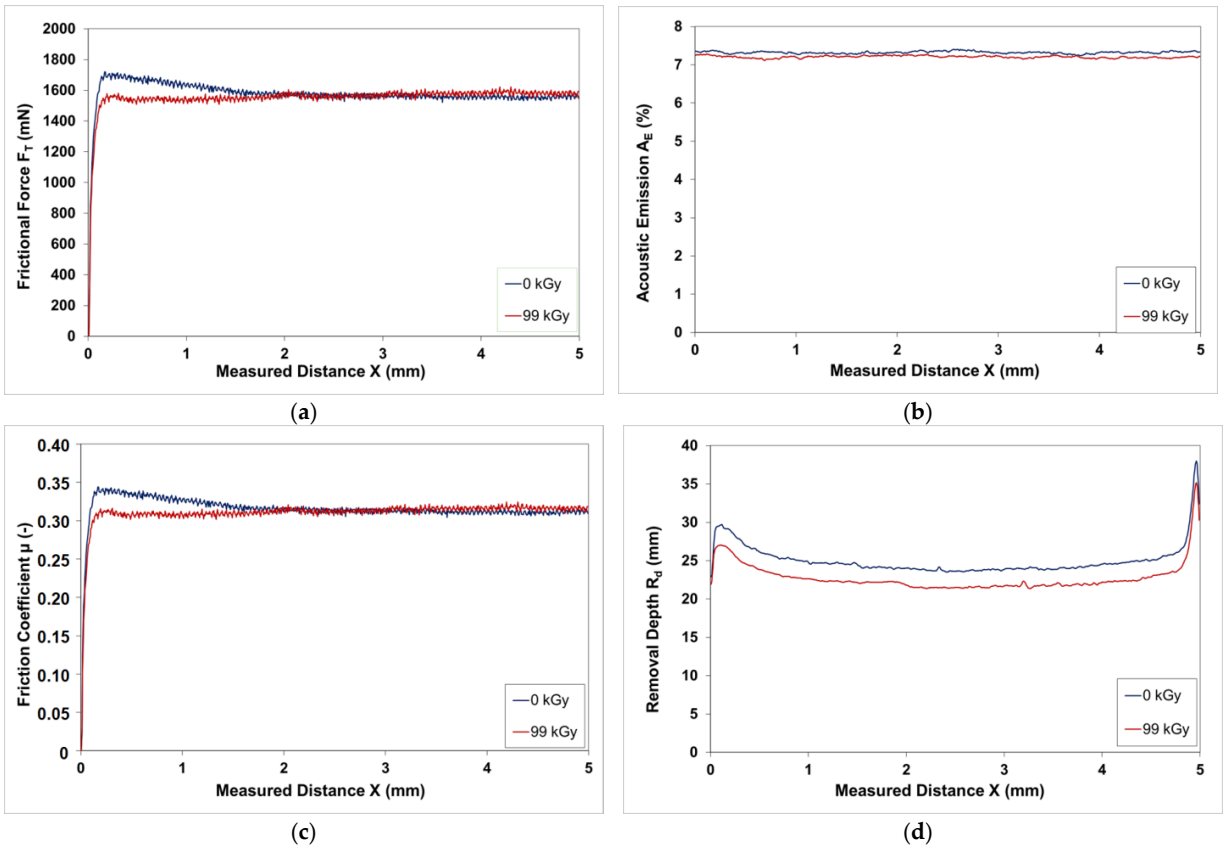

Figure 3. Tribological behaviors at a load of 1 N: (**a**) Frictional force; (**b**) Acoustic emission; (**c**) Friction coefficient; (**d**) Removal depth.

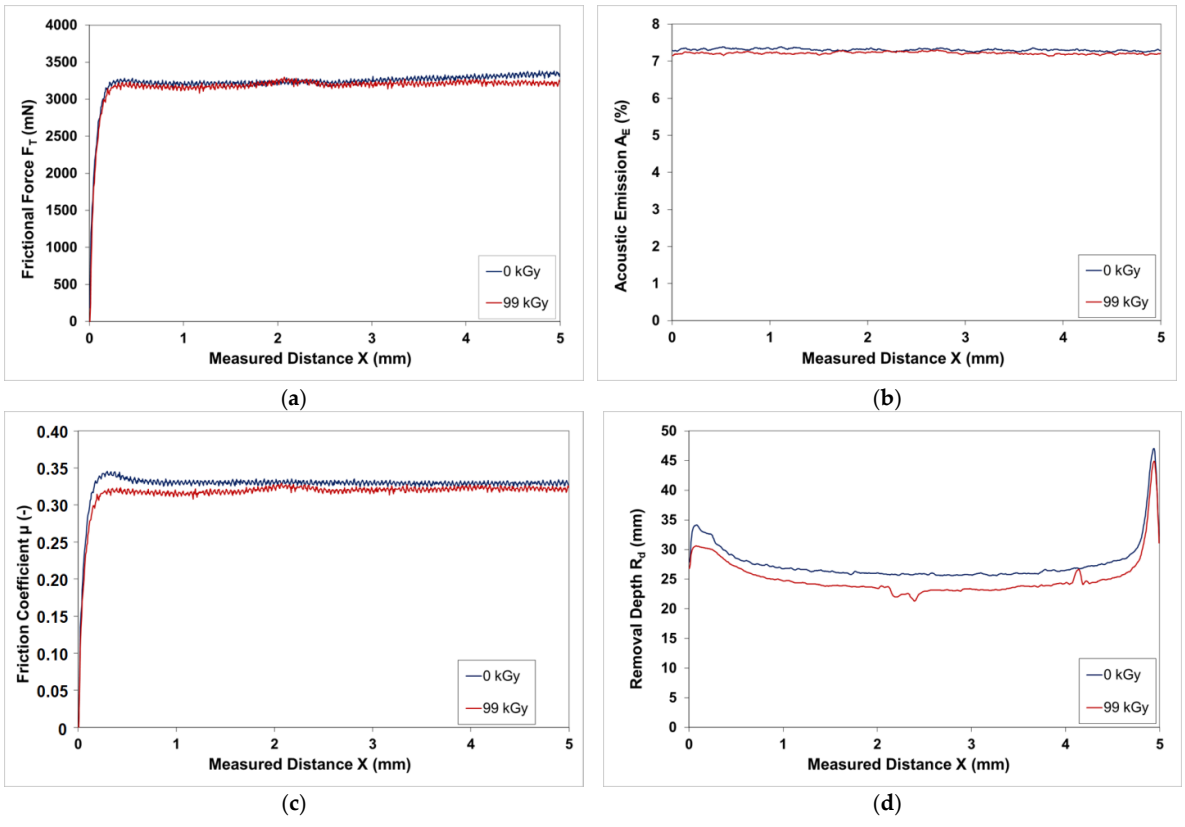

Figure 4. Tribological behaviors at a load of 5 N: (**a**) Frictional force; (**b**) Acoustic emission; (**c**) Friction coefficient; (**d**) Removal depth.

Table 5. Tribological behaviors at a loading force of 0.5 N.

Properties	Statistical Parameters	Irradiation Doses (kGy)						
		0	**33**	**66**	**99**	**132**	**165**	**198**
F_T (mN)	$\bar{x}$	279.04	274.53	267.21	267.06	264.47	264.84	271.23
	s	6.65	6.20	10.88	6.74	5.18	5.26	5.73
A_E (%)	$\bar{x}$	7.23	7.26	7.30	7.25	7.16	7.14	6.84
	s	0.03	0.03	0.03	0.03	0.02	0.03	0.03
μ (-)	$\bar{x}$	0.28	0.27	0.27	0.26	0.26	0.27	0.27
	s	0.01	0.01	0.01	0.01	0.01	0.01	0.01
R_d (mm)	$\bar{x}$	9.02	8.72	8.67	8.43	8.60	8.72	9.04
	s	0.45	0.42	0.41	0.37	0.45	0.41	0.38

Table 6. Tribological behaviors at a loading force of 1 N.

Properties	Statistical Parameters	Irradiation Doses (kGy)						
		0	**33**	**66**	**99**	**132**	**165**	**198**
F_T (mN)	$\bar{x}$	1579.80	1583.09	1562.29	1565.22	1547.28	1545.28	1556.70
	s	33.98	41.32	15.42	20.13	15.80	25.97	19.42
A_E (%)	$\bar{x}$	7.32	7.28	7.27	7.20	7.18	7.15	6.82
	s	0.03	0.03	0.03	0.03	0.03	0.04	0.02
μ (-)	$\bar{x}$	0.32	0.32	0.31	0.30	0.31	0.31	0.31
	s	0.01	0.01	0.00	0.00	0.00	0.01	0.00
R_d (mm)	$\bar{x}$	24.71	22.51	21.91	22.46	21.79	21.56	21.85
	s	1.75	1.76	1.66	1.68	1.85	1.65	1.63

Table 7 and Figure 4 show the results of the tribological behaviors of irradiated HDPE under an applied load of 5 N. The results show similar trends as under loads of 0.5 N and 1 N. The application of electron radiation improved all tribological behaviors. For example, a friction coefficient of 0.33 was measured for non-irradiated HDPE, and a friction coefficient of 0.31 was measured with an applied dose of 99 kGy. The radiation improved the friction coefficient by 7%. Higher radiation doses lead to a deterioration in tribological behaviors due to the onset of a degradation process.

Table 7. Tribological behaviors at a loading force of 5 N.

Properties	Statistical Parameters	Irradiation Doses (kGy)						
		0	**33**	**66**	**99**	**132**	**165**	**198**
F_T (mN)	$\bar{x}$	3299.60	3255.08	3183.01	3203.64	3180.27	3179.80	3158.23
	s	23.11	48.98	32.73	33.52	28.39	38.44	38.78
A_E (%)	$\bar{x}$	7.31	7.29	7.29	7.22	7.17	7.10	6.86
	s	0.03	0.03	0.02	0.03	0.03	0.03	0.03
μ (-)	$\bar{x}$	0.33	0.33	0.32	0.31	0.31	0.32	0.32
	s	0.00	0.00	0.00	0.00	0.00	0.00	0.00
R_d (mm)	$\bar{x}$	27.13	25.01	24.54	24.69	24.84	24.92	23.95
	s	3.05	3.04	2.98	3.11	3.19	2.71	2.89

When comparing tribological behaviors at different load forces, it can be stated that tribological behaviors show higher values when measured at higher applied loads. When measured at a load force of 0.5 N, the coefficient of friction was 0.26 for a radiation dose of 99 kGy. At a load force of 1 N, the coefficient of friction for HDPE irradiated at 99 kGy was 0.30, and at a load force of 5 N, the coefficient of friction for HDPE irradiated at 99 kGy was 0.31. The difference between the applied load forces was up to 19%. This is due to the surface quality, which negatively affects the results at low load forces (0.5 N). There was a slight difference of 3% between the applied loads of 1 N and 5 N. Higher applied loads

cancel out the influence of surface quality, and therefore applied loads of 1 N and higher can be recommended.

Previous studies by Maňas et al. [32] and Bednařík et al. [33] have shown that electron irradiation enhances surface wettability, as evidenced by a reduction in the wetting contact angle, which in turn contributes to a lower coefficient of friction in irradiated HDPE. An increase in radiation dose further promotes surface wettability, a trend that is consistent with the observed improvement in the tribological performance of HDPE following irradiation.

The tribological behaviors of the tested HDPE improved due to radiation modification, resulting in improved resistance of the surface layer to mechanical damage. Due to these changes, irradiated HDPE can be used in demanding applications that require high surface resistance to long-term wear. This improvement is due to a change in structure (Section 3.4), which also results in improved micro-mechanical behaviors (Section 3.3). Tribological and micro-mechanical behaviors show similar trends and improvements due to the application of electron radiation to the tested HDPE.

3.3. Micro-Mechanical Behaviors

Micro-mechanical behaviors (indentation hardness, indentation modulus, indentation creep, and depth) were measured at three applied loads of 0.5 N, 1 N, and 5 N in order to eliminate the influence of surface quality. Furthermore, micro-mechanical behaviors were measured in cross-sections to describe the influence of electron radiation across the entire thickness of the sample and also the influence of radiation on the structure itself.

3.3.1. Micro-Mechanical Behaviors Under Different Indentation Load (0.5 N, 1 N and 5 N)

Figure 5 and Tables A2–A4 show the micro-mechanical behaviors (indentation hardness, indentation modulus, indentation creep, and depth) at three load sizes (0.5 N, 1 N, and 5 N) of electron-beam modified HDPE. Different loading forces were selected to examine the impact of electron irradiation on the depth of radiation penetration. Figure 5a shows the dependence of indentation force on indentation depth (F-h). For better clarity, curves were selected only for non-irradiated HDPE and HDPE irradiated with a dose of 132 kGy, which showed the highest values of micro-mechanical behaviors at all indentation loads. The indentation curves (F-h) describe the course of the indentation measurement, both during the loading cycle and during the unloading of the indenter. The micro-mechanical behaviors are evaluated based on these characteristics. Both curves show that the material behaves elastic–plastically, which is reflected in the measured parameters.

Figure 5b shows the measured indentation depths of irradiated HDPE at three loading forces (0.5 N, 1 N, and 5 N). At a load of 0.5 N, the indentation depth measured for non-irradiated HDPE was 26.2 μm, and for HDPE subjected to a radiation dose of 99 kGy, the depth measured was 23.9 μm. At a load force of 1 N, the indentation depth measured for non-irradiated HDPE was 36.0 μm and for irradiated HDPE with a dose of 99 kGy was 33.9 μm. At a load of 5 N, the indentation depth measured for non-irradiated HDPE was 77.9 μm and for irradiated HDPE with a dose of 132 kGy, it was 75.0 μm. As can be seen in Figure 4b, the micro-mechanical behaviors were measured in the range of depths from approx. 26 μm to 78 μm, which allows for a better assessment of the effect of radiation on the resulting material.

Figure 5c shows a graphical evaluation of the indentation hardness of irradiated HDPE for three load sizes. The indentation hardness values are influenced by the load size. The indentation hardness value increases with increasing load. For all loads, the maximum indentation hardness values were measured at radiation doses of 99 kGy and 132 kGy. When measuring with a load force of 0.5 N, the indentation hardness of non-irradiated HDPE was measured at 36.5 MPa. When electron radiation was applied, there was a

significant increase in indentation hardness, up to a value of 43.2 MPa at a radiation dose of 99 kGy. The difference between non-irradiated and irradiated HDPE was 18%. Higher radiation doses led to the onset of material degradation due to the high radiation dose. At a dose of 198 kGy, an indentation hardness of 40.5 MPa was measured. When measured with a higher indentation force of 1 N, an increase in indentation hardness was observed. An indentation hardness of 37.9 MPa was measured for unirradiated HDPE. When electron radiation was applied, a significant improvement in indentation hardness was observed, with a maximum at a radiation dose of 132 kGy, when the indentation hardness was 42.9 MPa. The difference between pure HDPE and radiation-modified HDPE was a 13% increase in indentation hardness. Again, increasing the radiation dose resulted in a reduction in indentation hardness to 40.6 MPa, which is caused by the onset of material degradation due to high radiation doses. When measured with a load of 5 N, non-irradiated HDPE exhibited an indentation hardness of 40.0 MPa, and with the application of electron radiation (dose of 132 kGy), an indentation hardness of 43.0 MPa was measured. Thanks to the modification of electron radiation on HDPE, the indentation hardness improved by 8%. At higher radiation doses, indentation hardness decreased to 41.8 MPa (dose of 198 kGy). When comparing the indentation hardness results at all loading forces (0.5 N, 1 N, 5 N), it can be stated that the higher the loading force, the higher the hardness values. This is also evidenced by the depth of the indentation achieved, which was measured at 26.2 μm under an applied load of 0.5 N and 77.9 μm under a load of 5 N. This is caused by the penetration of electron radiation through the material and the formation of a 3D network in the structure. The difference between the indentation hardness measured at a load of 0.5 N and 5 N is 10%. This indicates that further below the surface of the specimen, the structure is more extensively cross-linked.

Figure 5d shows the indentation modulus of electron-beam modified HDPE under three loading forces (0.5 N, 1 N, and 5 N). The indentation modulus indicates the stiffness of the material, i.e., its resistance to elastic deformation (deformation) under load. As can be seen from the figure, the indentation modulus increases with the dose of electron radiation for all loading forces. When measured with an applied load of 0.5 N, the non-irradiated HDPE had an indentation modulus of 1.28 GPa. With increasing doses of electron radiation, the indentation modulus increased, reaching a maximum of 1.57 GPa at a radiation dose of 99 kGy. Higher radiation doses showed a slight decrease in the indentation modulus to 1.39 GPa at a dose of 198 kGy, which is again due to the onset of degradation due to high radiation intensity. At a loading force of 0.5 N, the indentation modulus improved by 23% due to irradiation. Similar trends were observed at an applied load of 1 N. Non-irradiated HDPE exhibited an indentation modulus of 1.33 GPa, and with the application of electron radiation, the indentation modulus increased to 1.54 GPa at a radiation dose of 99 kGy. The indentation modulus improved by 16% due to irradiation. With increasing radiation dose, indentation hardness decreased to 1.40 GPa. At a maximum load force of 5 N, non-irradiated HDPE exhibited an indentation modulus of 1.32 GPa, and the application of electron radiation improved the indentation modulus to 1.60 GPa at a radiation dose of 99 kGy. Higher radiation doses again began to cause slight degradation of the structure, and the values decreased to 1.48 GPa. Thanks to the application of electron radiation, the indentation modulus improved by 21%. When comparing the results of the indentation modulus at different loading forces (0.5 N, 1 N, and 5 N), it can be stated that between the loading forces of 0.5 N and 5 N, the indentation modulus increased by up to 10%. The lower values of the indentation modulus at lower loads are due to the higher percentage of cross-linked structure caused by electron irradiation.

Figure 5e shows the indentation characteristics of the dependence of indentation depth on indentation time, which are used to determine indentation creep. Indentation creep of

a material is a time-dependent plastic deformation in which the material is permanently deformed, stretched, or compressed under constant load, even if it is below the yield point. This is a basic mechanism of material aging, which is especially important for components operating under long-term load, where atoms in the material rearrange and cause it to flow. Figure 5f shows the indentation creep of electron-irradiated modified HDPE under three applied loads (0.5 N, 1 N, and 5 N). At an applied load of 0.5 N, the indentation creep of non-irradiated HDPE was 16.3%. Following radiation treatment, the indentation creep improved to 14.3% at a radiation dose of 66 kGy; higher radiation doses showed similar values. Indentation creep improved by 14%. At a load of 1 N, the indentation creep of unirradiated HDPE was 16.0%, and following electron irradiation, indentation creep improved to 14.5% at a radiation dose of 198 kGy. At an applied load of 5 N, non-irradiated HDPE showed values of 15.1%, and with the application of electron radiation, there was an improvement to 14.1% (dose of 165 kGy). When comparing load forces of 0.5 N and 5 N, there was an 8% improvement in indentation creep.

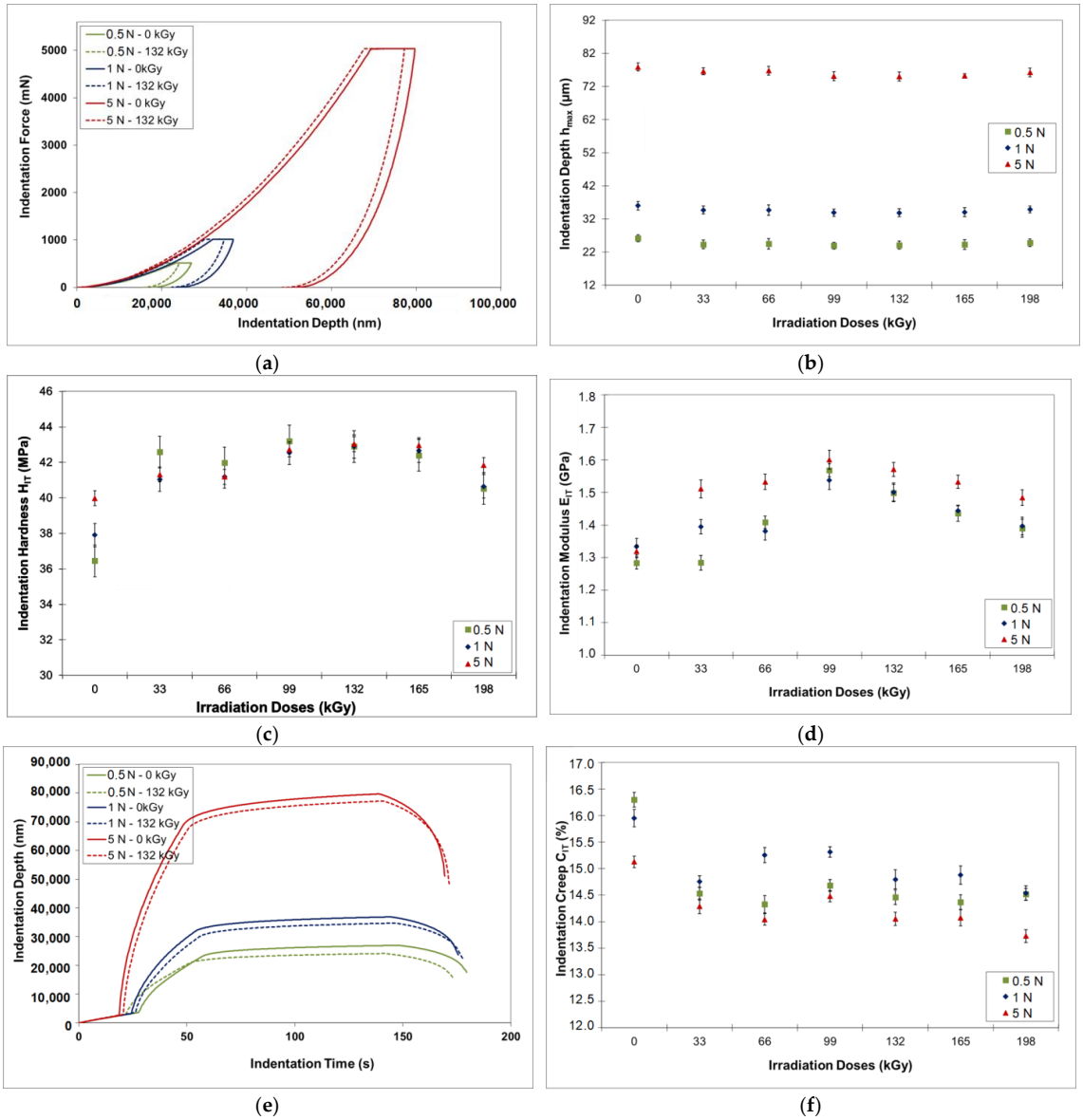

Figure 5. Micro-mechanical behaviors of modified HDPE under applied loads of 0.5 N, 1 N, 5 N: (**a**) indentation load dependence on indentation depth; (**b**) Indentation depth; (**c**) Indentation hardness; (**d**) Indentation modulus; (**e**) Indentation depth dependence on indentation time (creep); (**f**) Indentation creep.

It can be stated that electron beam modification improves the micro-mechanical behaviors of HDPE. The optimal dose appears to be 99 kGy to 132 kGy, at which all monitored parameters showed significant improvement. Higher radiation doses show a slight decrease in micro-mechanical behaviors, which is caused by the onset of degradation of the HDPE structure due to high polymer loading with electron radiation. These results complement and confirm the trends found in the measurement of tribological behaviors (Section 3.2).

3.3.2. Micro-Mechanical Behaviors in Different Layers Under the Surface

To confirm the effect of electron radiation on the entire thickness of the tested HDPE, cuts were made in individual layers below the surface (0.6 mm, 1.3 mm, 2 mm, 2.7 mm, 3.4 m below the surface), where the micro-mechanical behaviors were tested.

Figure 6 and Tables A5–A11 show the micro-mechanical behaviors of irradiated HDPE, which are measured in cuts so that the effect of radiation across the entire thickness of the sample can be captured.

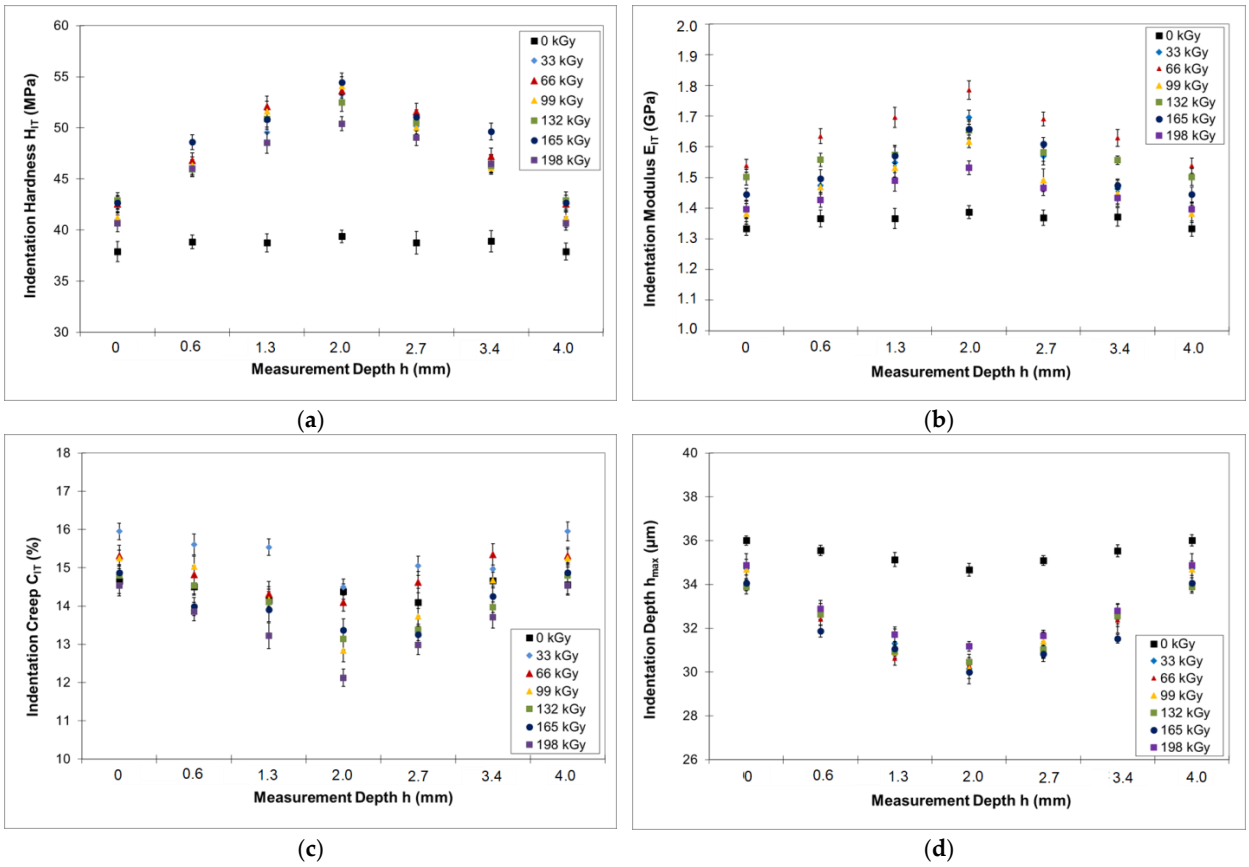

Figure 6. Micro-mechanical behaviors of modified HDPE in subsurface layers: (**a**) Indentation hardness; (**b**) Indentation modulus; (**c**) Indentation creep; (**d**) Indentation depth.

Figure 6a shows the indentation hardness results at different depths of irradiated HDPE. The figure demonstrates that the indentation hardness increases from the surface of the tested body (0 mm) to the center of the tested body (2 mm) for all radiation doses. For non-irradiated HDPE, constant values were measured across the entire thickness of the tested body (39 MPa). Electron irradiation caused a significant increase in indentation hardness toward the center of the sample for all applied doses. For example, at a radiation dose of 99 kGy, the surface of the sample (0 mm) showed an indentation hardness of 41 MPa, and towards the center (2 mm), the indentation hardness increased to 54 MPa. The difference through the cross-section of the tested HDPE was 32%. The trend was similar

for other radiation doses. On the surface of the sample (0 mm), the difference between non-irradiated and irradiated HDPE at a dose of 99 kGy was about 6%, and in the center (2 mm), this difference was significant, amounting to 39%.

Similar results were measured for the indentation modulus (Figure 6b). The non-irradiated HDPE showed constant indentation modulus values across the entire thickness of the tested material, around 1.36 GPa. Due to the effect of electron radiation, an increase in the indentation modulus was observed from the surface (0 mm) to the center of the tested HDPE (2 mm). At a radiation dose of 66 kGy, values of 1.52 GPa were measured at the surface of the tested HDPE (0 mm) and values of 1.79 GPa were measured at the center of the tested HDPE (2 mm). The improvement in the indentation modulus between the surface and the center of the tested irradiated HDPE was 18%. A similar trend between the surface and the center was measured for all radiation doses. When comparing non-irradiated and irradiated HDPE (dose 66 kGy), it can be stated that the difference in the indentation modulus was 12% on the surface (0 mm) and up to 32% in the center (2 mm). The results correlate with the indentation hardness data, where the trends in growth towards the center were similar.

Figure 6c presents the indentation creep measurements of irradiated HDPE at various depths below the sample surface. For non-irradiated HDPE, constant indentation creep values of 14.3% were measured across the entire thickness. The best indentation creep values were exhibited by HDPE irradiated at 198 kGy, where indentation creep of 14.4% was measured at the surface (0 mm) and improved to 12.1% towards the center (2 mm). The difference between the surface and the center of the tested HDPE was 19%. The difference between non-irradiated and irradiated HDPE in the center of the sample (2 mm) was 20%. Other radiation doses showed similar trends in the improvement of indentation creep towards deeper layers.

The indentation depth corresponded to the results of indentation hardness, indentation modulus, and indentation creep measurements, as shown in Figure 6d. The non-irradiated HDPE had an indentation depth of approximately 36 μm across its entire thickness. Due to the application of electron radiation, the depth at the surface was around 34 μm, and towards the center, the depth decreased to 30 μm. These depths correspond to the measured micro-mechanical behaviors.

The results of micro-mechanical behaviors obtained by the indentation method (DSI) across the sample cross-section correspond to the measurement of tribological behaviors (Section 3.2) and micro-mechanical behaviors at different loading forces (Section 3.3.1), as well as with structural measurements performed by gel testing and wide-angle X-ray diffraction (Section 3.4). As observed, electron irradiation positively influences the properties throughout the full thickness of the material. The measured micro-mechanical behaviors were lower at the surface of the HDPE samples compared to the interior, reflecting variations in crystallinity and gel content. Gel content and crystallinity have a significant effect on the mechanical and tribological behaviors that were measured.

As the measurement results show, the design of the microhardness tester, high positioning accuracy, and insignificant influence of the surroundings of the indentation make the DSI method ideal for studying the properties of modified HDPE or changes in properties caused throughout the thickness of the products. The method used is capable of recording subtle alterations in mechanical behaviors throughout the cross-section of their thickness. An increase in hardness relative to the center of the sample was measured for almost all polymers. Owing to the high precision of the indenter and measurement system, both subtle variations across the full cross-section and more pronounced differences could be captured.

As previous results show, the tribological and micro-mechanical behaviors of electron-beam modified HDPE show significant improvements in these properties, which confirms the findings of the authors in their publications [34–38]. In their publications, the authors confirm that electron irradiation has a positive effect on HDPE in terms of structural changes (crystallinity, cross-linking content, etc.), which significantly improves its useful properties and practical applications.

3.4. Structural Behaviors

Electron irradiation strongly affects structural changes in the tested HDPE, which were measured using a gel test and wide-angle X-ray diffraction. The structural results have a fundamental impact on confirming the changes that were detected using tribological and micro-mechanical tests and the behaviors that were identified.

3.4.1. Gel Content

The gel test was performed to quantify the non-filterable fraction—the gel—in the material according to EN ISO 579. Figure 7 and Table A12 present the gel content of HDPE as a function of the applied radiation dose. As illustrated, the gel fraction reached its maximum in HDPE irradiated at the highest dose of 198 kGy, while no measurable gel content was detected for doses up to 66 kGy. Notably, measurements of tribological and micro-mechanical behaviors indicated that even HDPE irradiated at lower doses exhibited detectable changes. The accuracy of gel content determination depends strongly on the robustness of the filter screen, meaning that small "microgels" formed at lower radiation doses can pass through the filter and are therefore not accounted for in the total gel content. Nevertheless, these microgels already contribute to changes in the material's measured properties. A marked increase in gel content (55%) was observed at 99 kGy, coinciding with significant modifications in tribological and micro-mechanical behavior. At higher doses of 132–198 kGy, gel content increased slightly further, reaching approximately 66%. Overall, the fraction of cross-linked material correlates closely with observed changes in the tribological and micro-mechanical behaviors of HDPE.

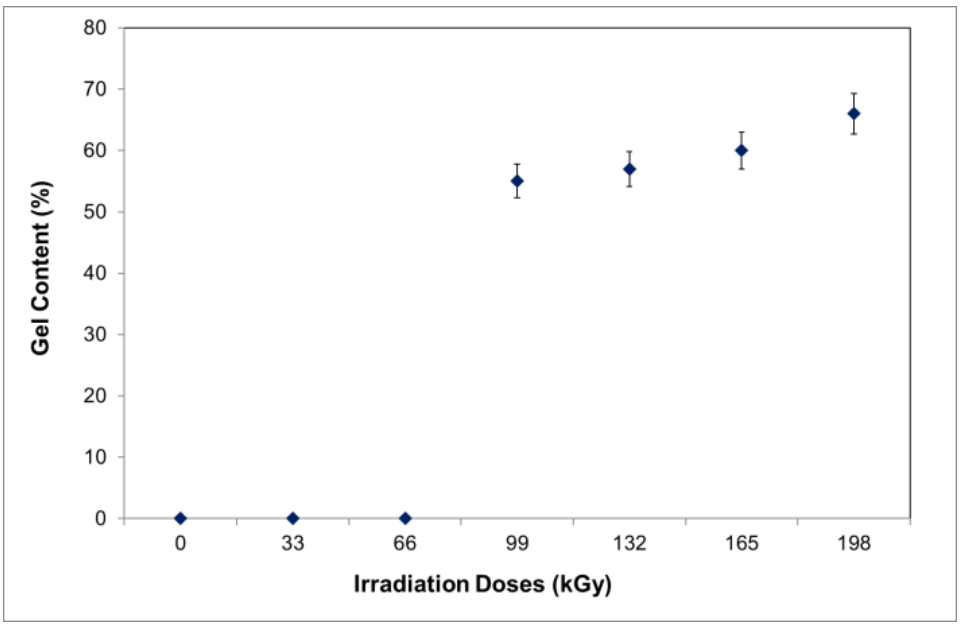

Figure 7. Gel test of modified HDPE.

3.4.2. Wide-Angle X-Ray Diffraction

Using wide-angle X-ray diffraction, the content of the crystalline and amorphous phases was measured both in the surface layer (0 mm) and in the center of the tested body (2 mm), as shown in Figure 8.

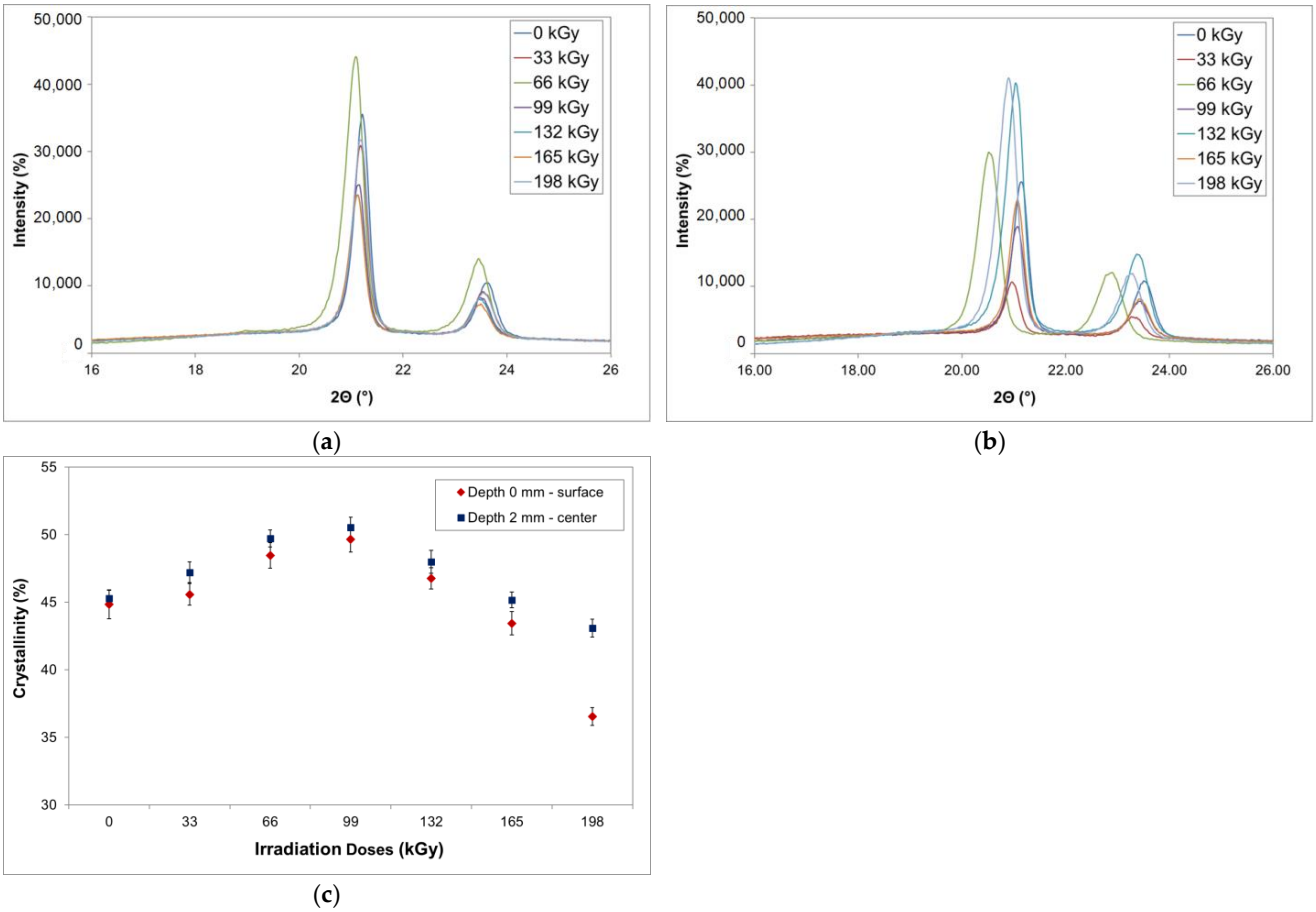

Figure 8. Wide-angle X-ray diffraction of modified HDPE: (**a**) surface of sample (0 mm); (**b**) center of sample (2 mm); (**c**) Crystallinity on the surface and in the center of the tested HDPE.

X-ray diffraction was performed to determine the effect of radiation cross-linking on the crystalline structure and degree of crystallinity of irradiated HDPE material. Crystallinity is determined by measuring the areas of the amorphous and crystalline fractions of the sample studied, which are shown in Figure 8a,b.

The effect of electron radiation on the crystalline and amorphous regions of polymers (HDPE) varies significantly depending on the degree of order in their structure. Electron irradiation initiates chemical processes that can either improve properties (cross-linking) or deteriorate them (degradation). In HDPE, electron radiation causes specific structural changes that manifest themselves differently in the crystalline and amorphous regions due to the different mobility of the chains. The amorphous phase is crucial for the radiation cross-linking process in HDPE. In amorphous parts, macromolecular chains are arranged irregularly ("in clumps"), which facilitates the movement of radicals and chemical reactions. The amorphous phase is the main site where radiation cross-linking (formation of a 3D network) occurs. Free radicals formed by irradiation move more easily in the disordered amorphous region, leading to their mutual reactions and the formation of strong cross-links (C–C) between chains. This increases the density of the network, which increases strength and creep resistance. The density of the amorphous phase increases slightly with increasing radiation dose due to the formation of these bonds, resulting in an increase in crystallinity. Crystals are densely

arranged structures that offer greater resistance to the penetration and movement of induced radicals. Crystalline lamellae in HDPE make up approximately 70% of the volume and act as a barrier to chemical changes. Inside the crystals, the chains are tightly arranged, which prevents their movement. Radicals remain "trapped" here and minimal cross-linking occurs. At very high radiation doses, the crystal lattice is disrupted (amorphization) and defects occur. This leads to a decrease in the degree of crystallinity (material degradation) and a reduction in mechanical properties. The authors describe the confirmation of the effect of radiation on the change in crystallinity and thus also on mechanical properties in their works [39–41]. Figure 8c and Table A13 show the results of the crystalline phase content in irradiated HDPE, which were measured both in the surface layer and in the center of the tested HDPE (2 mm). The surface layer showed lower crystallinity values than in the center (2 mm) of the tested HDPE. In the surface layer (0 mm), crystallinity of 44.9% was measured for non-irradiated HDPE. With increasing radiation dose, crystallinity increased to a maximum at a radiation dose of 99 kGy, where crystallinity of 49.7% was measured. The difference in crystallinity increase between non-irradiated and irradiated HDPE was 11%. Higher radiation doses led to a decrease in crystallinity, which is caused by material degradation due to high radiation intensity. The decrease in crystallinity at higher radiation doses corresponds to a decrease in tribological and micro-mechanical behaviors. In the center of the tested unirradiated HDPE, crystallinity of 45.1% was measured. At a radiation dose of 99 kGy, a maximum crystallinity of 50.6% was also measured. The increase in crystallinity between non-irradiated and irradiated HDPE was 12%. Again, higher radiation doses led to degradation processes and thus to a decrease in crystallinity. When comparing the surface layer (0 mm) and the layer in the center (2 mm), it can be stated that the crystallinity of non-irradiated HDPE was similar (around 45%), but when electron radiation with a dose of 99 kGy was applied, the difference between the surface (0 mm) and the center (2 mm) was significant. This suggests that the central region of the tested HDPE (2 mm) exhibits a higher degree of crystallization than the surface (0 mm). This finding corresponds to the measurement of gel content (Figure 7), where the crystalline phase content and gel content increase with increasing radiation dose. Network density does not increase proportionally with radiation dose because degradation processes occur concurrently with cross-linking, leading to a decline in both cross-linking degree and crystallinity. This behavior is corroborated by the observed micro-mechanical and tribological behaviors in various subsurface layers.

An important finding of this work is that, using an instrumented hardness test (DSI), it is possible to detect changes in structure (crystallinity and gel content) that are reflected in the resulting tribological and micro-mechanical behaviors, even in different layers of the tested HDPE. The results show that electron radiation can shift the properties of a commodity polymer such as HDPE to the level of a more expensive engineering polymer at minimal cost for irradiating the sample. The micro-mechanical and tribological behaviors predestine modified HDPE for wide use in areas where higher wear resistance is required. Conventional HDPE exhibits limited performance in meeting these criteria. Exposure to electron radiation markedly enhanced both the tribological and micro-mechanical behaviors of the material, which is associated with structural changes, including variations in crystallinity and gel content. These observations are consistent with findings reported by other authors [33–38].

4. Conclusions

This work demonstrates that electron-beam irradiation represents an effective and controllable strategy for transforming commodity HDPE into a material with characteristics approaching those of advanced engineering polymers. The key scientific contribution lies in establishing a clear structure–property relationship across the entire cross-section of

the material, showing that radiation-induced crosslinking and crystallinity evolution are not confined to the surface but develop heterogeneously through the bulk. This finding extends current understanding, which is predominantly limited to near-surface analyses, and highlights the importance of considering depth-dependent structural gradients when evaluating irradiated polymers.

The results confirm that an optimal irradiation window exists in which crosslinking and crystalline rearrangement act synergistically to enhance stiffness, wear resistance, and time-dependent deformation behavior, while avoiding the dominance of degradation mechanisms. Beyond this window, chain scission and structural disruption progressively limit further performance gains, underscoring the balance between crosslinking and degradation as the governing principle of radiation modification in HDPE.

A further significant outcome is the validation of depth-sensing indentation as a sensitive and reliable tool for detecting subtle radiation-induced structural changes and correlating them with tribological performance throughout the material thickness. This methodological approach provides a robust framework for linking micro-mechanical response to underlying morphology, enabling more predictive assessment of irradiated polymer systems.

From an application perspective, the demonstrated ability to tailor bulk and surface properties through electron irradiation offers a cost-efficient pathway for expanding the functional range of HDPE in wear-critical and mechanically demanding applications. More broadly, the presented findings contribute to the global body of knowledge on radiation-modified polymers by providing comprehensive, cross-sectional insight into how irradiation governs structure–property relationships, thereby supporting the rational design of high-performance polymer components using established, economically favorable materials.

Author Contributions: Conceptualization, M.O.; methodology, M.O.; validation, A.C., K.F. and M.S.; formal analysis, A.C. and A.P.; investigation, M.S.; resources, M.O.; data curation, A.C., A.P. and K.F.; writing—original draft preparation, M.O.; writing—review and editing, M.O.; visualization, M.O.; supervision, M.O.; project administration, M.S. All authors have read and agreed to the published version of the manuscript.

Funding: This research was conducted with the support of the Internal Grant Agency of Tomas Bata University in Zlín, supported under project no. IGA/FT/2026/001.

Institutional Review Board Statement: Not applicable.

Data Availability Statement: The original contributions presented in this study are included in the article. Further inquiries can be directed to the corresponding author(s).

Conflicts of Interest: The authors declare no conflicts of interest.

Appendix A

Table A1. Surface quality Ra (statistical parameters).

Properties	Statistical Parameters	Irradiation Doses (kGy)						
		0	**33**	**66**	**99**	**132**	**165**	**198**
Surface quality Ra (μm)	$\bar{x}$	0.66	0.68	0.65	0.68	0.65	0.62	0.64
	s	0.03	0.02	0.02	0.02	0.02	0.02	0.02

Table A2. Micro-mechanical behavior (statistical parameters) under a load of 0.5 N.

Properties	Statistical Parameters	Irradiation Doses						
		0	**33**	**66**	**99**	**132**	**165**	**198**
H_{IT} (MPa)	$\bar{x}$	36.46	42.58	41.97	43.20	42.89	42.39	40.52
	s	0.46	0.40	0.49	0.51	0.50	0.25	0.49
E_{IT} (GPa)	$\bar{x}$	1.28	1.28	1.41	1.57	1.50	1.44	1.39
	s	0.02	0.03	0.02	0.03	0.02	0.02	0.02
C_{IT} (%)	$\bar{x}$	16.30	14.53	14.33	14.68	14.46	14.37	14.52
	s	0.11	0.14	0.11	0.10	0.13	0.15	0.12
h_{max} (µm)	$\bar{x}$	26.15	24.31	24.45	23.92	24.11	24.30	24.81
	s	1.23	1.06	1.31	1.37	1.33	0.67	1.31

Table A3. Micro-mechanical behavior (statistical parameters) under a load of 1 N.

Properties	Statistical Parameters	Irradiation Doses						
		0	**33**	**66**	**99**	**132**	**165**	**198**
H_{IT} (MPa)	$\bar{x}$	37.90	41.03	41.19	42.54	42.90	42.66	40.65
	s	0.50	0.44	0.61	0.41	0.45	0.50	0.39
E_{IT} (GPa)	$\bar{x}$	1.33	1.39	1.38	1.54	1.50	1.44	1.40
	s	0.03	0.02	0.03	0.03	0.03	0.01	0.03
C_{IT} (%)	$\bar{x}$	15.95	14.76	15.26	15.32	14.80	14.88	14.54
	s	0.16	0.11	0.15	0.10	0.18	0.17	0.14
h_{max} (µm)	$\bar{x}$	36.01	34.73	34.69	33.93	33.89	34.06	34.87
	s	1.33	1.16	1.62	1.09	1.21	1.33	1.05

Table A4. Micro-mechanical behavior (statistical parameters) under a load of 5 N.

Properties	Statistical Parameters	Irradiation Doses (kGy)						
		0	**33**	**66**	**99**	**132**	**165**	**198**
H_{IT} (MPa)	$\bar{x}$	39.98	41.31	41.18	42.73	43.03	42.96	41.84
	s	0.40	0.50	0.59	0.38	0.46	0.54	0.45
E_{IT} (GPa)	$\bar{x}$	1.32	1.51	1.53	1.60	1.57	1.53	1.48
	s	0.02	0.02	0.02	0.02	0.03	0.02	0.03
C_{IT} (%)	$\bar{x}$	15.13	14.29	14.04	14.48	14.05	14.07	13.73
	s	0.14	0.12	0.16	0.11	0.14	0.14	0.11
h_{max} (µm)	$\bar{x}$	77.87	76.55	76.79	75.15	75.03	75.23	76.25
	s	1.06	1.33	1.58	1.01	1.22	1.45	1.19

Table A5. Micro-mechanical behavior (statistical parameters) depending on the measurement length for a radiation dose of 0 kGy.

Properties	Statistical Parameters	Measurement Depth (mm)						
		0.0	**0.6**	**1.3**	**2.0**	**2.7**	**3.4**	**4.0**
H_{IT} (MPa)	$\bar{x}$	37.90	38.83	38.75	39.38	38.76	38.90	37.90
	s	0.63	0.73	0.97	0.90	0.67	0.82	0.77
E_{IT} (GPa)	$\bar{x}$	1.33	1.37	1.37	1.39	1.37	1.37	1.33
	s	0.02	0.02	0.03	0.03	0.02	0.03	0.03
C_{IT} (%)	$\bar{x}$	14.66	14.51	14.15	14.38	14.10	14.66	14.56
	s	0.21	0.24	0.32	0.30	0.22	0.27	0.25
h_{max} (µm)	$\bar{x}$	36.01	35.55	35.13	34.67	35.10	35.54	36.01
	s	0.21	0.24	0.32	0.30	0.22	0.27	0.26

Table A6. Micro-mechanical behavior (statistical parameters) depending on the measurement length for a radiation dose of 33 kGy.

Properties	Statistical Parameters	Measurement Depth (mm)						
		0.0	**0.6**	**1.3**	**2.0**	**2.7**	**3.4**	**4.0**
H_{IT} (MPa)	$\bar{x}$	41.03	46.06	49.57	53.27	50.17	46.49	41.03
	s	0.61	0.83	1.01	0.89	0.63	0.61	0.72
E_{IT} (GPa)	$\bar{x}$	1.39	1.47	1.55	1.70	1.57	1.46	1.39
	s	0.02	0.03	0.03	0.03	0.02	0.02	0.02
C_{IT} (%)	$\bar{x}$	15.95	15.61	15.54	14.49	15.05	14.97	15.95
	s	0.20	0.28	0.33	0.29	0.21	0.20	0.24
h_{max} (µm)	$\bar{x}$	34.73	32.60	31.31	30.14	31.14	32.45	34.73
	s	0.20	0.28	0.34	0.30	0.21	0.20	0.24

Table A7. Micro-mechanical behavior (statistical parameters) depending on the measurement length for a radiation dose of 66 kGy.

Properties	Statistical Parameters	Measurement Depth (mm)						
		0.0	**0.6**	**1.3**	**2.0**	**2.7**	**3.4**	**4.0**
H_{IT} (MPa)	$\bar{x}$	42.54	46.81	52.10	53.61	51.57	47.19	42.54
	s	0.77	0.66	0.82	0.85	0.83	0.42	0.82
E_{IT} (GPa)	$\bar{x}$	1.54	1.63	1.70	1.78	1.69	1.63	1.54
	s	0.03	0.02	0.03	0.03	0.03	0.01	0.03
C_{IT} (%)	$\bar{x}$	15.32	14.82	14.31	14.09	14.62	15.35	15.32
	s	0.25	0.22	0.27	0.28	0.28	0.14	0.27
h_{max} (µm)	$\bar{x}$	33.93	32.40	30.63	30.27	30.96	32.38	33.93
	s	0.26	0.22	0.27	0.28	0.28	0.14	0.27

Table A8. Micro-mechanical behavior (statistical parameters) depending on the measurement length for a radiation dose of 99 kGy.

Properties	Statistical Parameters	Measurement Depth (mm)						
		0.0	**0.6**	**1.3**	**2.0**	**2.7**	**3.4**	**4.0**
H_{IT} (MPa)	$\bar{x}$	41.19	46.31	51.60	54.11	50.02	46.09	41.19
	s	0.83	0.73	1.01	0.68	0.75	0.83	0.65
E_{IT} (GPa)	$\bar{x}$	1.38	1.47	1.53	1.62	1.49	1.45	1.38
	s	0.03	0.02	0.03	0.02	0.03	0.03	0.02
C_{IT} (%)	$\bar{x}$	15.26	15.03	14.17	12.84	13.73	14.68	15.26
	s	0.28	0.24	0.33	0.22	0.25	0.28	0.22
h_{max} (µm)	$\bar{x}$	34.69	32.63	30.90	30.17	31.39	32.74	34.69
	s	99.00	0.28	0.24	0.34	0.23	0.25	0.28

Table A9. Micro-mechanical behavior (statistical parameters) depending on the measurement length for a radiation dose of 132 kGy.

Properties	Statistical Parameters	Measurement Depth (mm)						
		0.0	**0.6**	**1.3**	**2.0**	**2.7**	**3.4**	**4.0**
H_{IT} (MPa)	$\bar{x}$	42.90	45.93	50.88	52.46	50.52	46.30	42.90
	s	0.66	0.83	0.99	0.63	0.76	0.91	0.75
E_{IT} (GPa)	$\bar{x}$	1.50	1.56	1.57	1.65	1.58	1.56	1.50
	s	0.02	0.03	0.03	0.02	0.03	0.03	0.02
C_{IT} (%)	$\bar{x}$	14.80	14.54	14.11	13.14	13.38	13.97	14.80
	s	0.22	0.28	0.22	0.21	0.25	0.30	0.25
h_{max} (µm)	$\bar{x}$	33.89	32.62	30.93	30.46	31.04	32.55	33.89
	s	0.22	0.28	0.33	0.21	0.25	0.30	0.25

Table A10. Micro-mechanical behavior (statistical parameters) depending on the measurement length for a radiation dose of 165 kGy.

Properties	Statistical Parameters	Measurement Depth (mm)						
		0.0	**0.6**	**1.3**	**2.0**	**2.7**	**3.4**	**4.0**
H_{IT} (MPa)	$\bar{x}$	42.66	48.61	50.84	54.44	51.08	49.64	42.66
	s	0.99	0.67	0.88	0.60	1.10	1.05	0.83
E_{IT} (GPa)	$\bar{x}$	1.44	1.50	1.57	1.66	1.61	1.47	1.44
	s	0.03	0.02	0.03	0.02	0.04	0.03	0.03
C_{IT} (%)	$\bar{x}$	14.88	13.99	13.91	13.37	13.25	14.25	14.88
	s	0.33	0.22	0.29	0.20	0.36	0.35	0.28
h_{max} (µm)	$\bar{x}$	34.06	31.88	31.07	30.00	30.83	31.53	34.06
	s	0.33	0.22	0.29	0.20	0.37	0.35	0.28

Table A11. Micro-mechanical behavior (statistical parameters) depending on the measurement length for a radiation dose of 198 kGy.

Properties	Statistical Parameters	Measurement Depth (mm)						
		0.0	**0.6**	**1.3**	**2.0**	**2.7**	**3.4**	**4.0**
H_{IT} (MPa)	$\bar{x}$	40.65	46.01	48.52	50.41	49.03	46.48	40.65
	s	0.83	0.73	0.99	0.68	0.84	0.83	0.65
E_{IT} (GPa)	$\bar{x}$	1.40	1.43	1.49	1.53	1.47	1.43	1.40
	s	0.03	0.02	0.03	0.02	0.03	0.03	0.02
C_{IT} (%)	$\bar{x}$	14.54	13.86	13.22	12.12	12.98	13.70	14.54
	s	0.28	0.24	0.33	0.22	0.28	0.28	0.22
h_{max} (µm)	$\bar{x}$	34.87	32.88	31.71	31.17	31.65	32.80	34.87
	s	0.28	0.24	0.33	0.23	0.28	0.28	0.22

Table A12. Gel content (statistical parameters).

Properties	Statistical Parameters	Irradiation Doses (kGy)						
		0	**33**	**66**	**99**	**132**	**165**	**198**
Gel content (%)	$\bar{x}$	0.00	0.00	0.00	55.00	57.00	60.00	66.00
	s	0.00	0.00	0.00	0.99	1.03	1.02	1.02

Table A13. Crystallinity (statistical parameters).

Properties	Statistical Parameters	Irradiation Doses (kGy)						
		0	**33**	**66**	**99**	**132**	**165**	**198**
Crystallinity (%)—surface	$\bar{x}$	44.86	45.59	48.47	49.68	46.78	43.45	36.55
	s	1.07	0.80	0.96	0.96	0.79	0.86	0.66
Crystallinity (%)—center	$\bar{x}$	45.28	47.22	49.73	50.56	48.00	45.18	43.09
	s	0.63	0.77	0.63	0.75	0.86	0.59	0.66

References

1. Woods, R.J. *Applied Radiation Chemistry: Radiation Processing*; Wiley: New York, NY, USA, 1994; 535p.
2. Chapiro, A. *Radiation Chemistry of Polymeric Systems*; Interscience Publishers, John Wiley & Sons: New York, NY, USA, 1962; 712p.
3. Dole, M.; Matsuo, H. Analysis of molecular weight changes and gel da-ta of some irradiated vinyl polymers. *J. Chem. Phys.* **1963**, *38*, 3006–3009.
4. Singh, A. Irradiation of polyethylene: Some aspects of crosslinking and oxidative degradation. *Radiat. Phys. Chem.* **1999**, *56*, 375–380. [CrossRef]
5. Tamboli, S.M. Crosslinked polyethylene. *Indian J. Chem. Technol.* **2004**, *11*, 853–864.

6. Sun, K.; Chen, J.; Zha, H.; Sun, W.-F.; Chen, Y.; Luo, Z. Dynamic Thermomechanical Analysis on Water Tree Resistance of Crosslinked Polyethylene. *Materials* **2019**, *12*, 746. [CrossRef]
7. Ratnam, C.; Ramarad, S.; Khalid, M.; Rashid, S.; Mohamed, Z. Effect of Electron Beam Radiation on the Mechanical Properties of Low-Density Polyethylene (LDPE)/Waste Tire Dust (WTD) Blends. *Macromol. Symp.* **2015**, *353*, 47–54. [CrossRef]
8. Ovsik, M.; Manas, M.; Stanek, M.; Dockal, A.; Vanek, J.; Mizera, A.; Adamek, M.; Stoklasek, P. Polyamide Surface Layer Nano-Indentation and Thermal Properties Modified by Irradiation. *Materials* **2020**, *13*, 2915. [CrossRef] [PubMed]
9. Fisher, J.; McEwen, H.; Tipper, J.; Galvin, A.; Ingram, J.; Kamali, A.; Ingham, E. Wear, Debris, and Biologic Activity of Cross-linked Polyethylene in the Knee. *Clin. Orthop. Relat. Res.* **2004**, *428*, 114–119. [CrossRef] [PubMed]
10. D'Lima, D.; Hermida, J.; Chen, P.; Colwell, C. Polyethylene cross-linking by two different methods reduces acetabular liner wear in a hip joint wear simulator. *J. Orthop. Res.*® **2003**, *21*, 761–766. [CrossRef]
11. Cole, J.; Lemons, J.; Eberhardt, A. Gamma irradiation alters fatigue-crack behavior and fracture toughness in 1900H and GUR 1050 UHMWPE. *J. Biomed. Mater. Res.* **2002**, *63*, 559–566. [CrossRef]
12. Pruitt, L.; Ansari, F.; Kury, M.; Mehdizah, A.; Patten, E.; Huddlestein, J.; Ries, M. Clinical trade-offs in cross-linked ultrahigh-molecular-weight polyethylene used in total joint arthroplasty. *J. Biomed. Mater. Res. Part B Appl. Biomater.* **2013**, *101B*, 476–484. [CrossRef]
13. Medel, F.; Martínez-Morlanes, M.; Alonso, P.; Rubín, J.; Pascual, F.; Puértolas, J. Microstructure, thermooxidation and mechanical behavior of a novel highly linear, vitamin E stabilized, UHMWPE. *Mater. Sci. Eng. C* **2013**, *33*, 182–188. [CrossRef]
14. Seetala, N.; Tull-Walker, N.; Baburaj, A.; Zhou, J.; Wilkins, R.; Barnett, M. Positron Lifetime Studies of Irradiated Ultra-High Molecular Weight Polyethylene and Composites Made of Martian Regolith. *Mater. Sci. Forum* **2014**, *783–786*, 1585–1590. [CrossRef]
15. Ríos, R.; Puértolas, J.; Martínez-Nogués, V.; Martínez-Morlanes, M.; Pascual, F.; Banzo, J.; Medel, F. Mechanical behavior, microstructure and thermooxidation properties of sequentially crosslinked ultrahigh molecular weight polyethylenes. *J. Appl. Polym. Sci.* **2013**, *129*, 2518–2526. [CrossRef]
16. Svoboda, P.; Trivedi, K.; Stoklasa, K.; Svobodová, D.; Ougizawa, T. Study of crystallization behaviour of electron beam irradiated polypropylene and high-density polyethylene. *R. Soc. Open Sci.* **2021**, *8*, 202250. [CrossRef]
17. Xiong, D.; Ma, R.; Lin, J.; Wang, N.; Jin, Z. Tribological properties and structure of ultra-high molecular weight polyethylene after gamma irradiation. *Proc. Inst. Mech. Eng. Part J J. Eng. Tribol.* **2007**, *221*, 315–320. [CrossRef]
18. Khonakdar, H.; Jafari, S.; Taheri, M.; Wagenknecht, U.; Jehnichen, D.; Häußler, L. Thermal and wide angle X-ray analysis of chemically and radiation-crosslinked low and high density polyethylenes. *J. Appl. Polym. Sci.* **2006**, *100*, 3264–3271. [CrossRef]
19. Yamane, S.; Kyomoto, M.; Moro, T.; Watanabe, K.; Hashimoto, M.; Takatori, Y.; Ishihara, K. Effects of extra irradiation on surface and bulk properties of PMPC-grafted cross-linked polyethylene. *J. Biomed. Mater. Res. Part A* **2015**, *104*, 37–47. [CrossRef]
20. Kosumsupamala, K.; Puttaraksa, N.; Seki, H.; Nishikawa, H. Micro-scale irradiation-induced effects of polyethylene film by 1 MeV proton beam writing. *J. Micromech. Microeng.* **2025**, *35*, 095011. [CrossRef]
21. *EN ISO 527-2:2025*; Plastics—Determination of Tensile Properties, Part 2: Test Conditions for Moulding and Extrusion Plastics. ISO: Geneva, Switzerland, 2025.
22. *ČSN EN ISO 14577-1*; Metallic Materials—Instrumented Indentation Test for Hardness and Materials Parameters—Part 1: Test Method. ISO: Geneva, Switzerland, 2015.
23. *ČSN EN ISO 14577-2*; Metallic Materials—Instrumented Indentation Test for Hardness and Materials Parameters—Part 2: Verification and Calibration of Testing Machines. ISO: Geneva, Switzerland, 2015.
24. *ČSN EN ISO 14577-3*; Metallic Materials—Instrumented Indentation Test for Hardness and Materials Parameters—Part 3: Calibration of Reference Blocks. ISO: Geneva, Switzerland, 2015.
25. *ČSN EN ISO 14577-4*; Metallic Materials—Instrumented Indentation Test for Hardness and Materials Parameters—Part 4: Test Method for Metallic and Non-Metallic Coatings. ISO: Geneva, Switzerland, 2016.
26. Ovsik, M.; Stanek, M.; Dockal, A. Tribological and Micro-Mechanical Properties of Injected Polypropylene Modified by Electron Radiation. *Lubricants* **2023**, *11*, 296. [CrossRef]
27. Ovsik, M.; Manas, M.; Stanek, M.; Dockal, A.; Mizera, A.; Fluxa, P.; Bednarik, M.; Adamek, M. Nano-Mechanical Properties of Surface Layers of Polyethylene Modified by Irradiation. *Materials* **2020**, *13*, 929. [CrossRef] [PubMed]
28. *EN ISO 579:2013*; Coke—Determination of Total Moisture. ISO: Geneva, Switzerland, 2013.
29. Huynh, N.P.; Chung, K.H. Effect of Counter Material on Tribological Properties of CoCrMoSi Alloy. *Tribol. Lett.* **2022**, *70*, 40. [CrossRef]
30. Von Frieandt, L.; Fallqvist, M.; Larsson, T.; Lindahl, E.; Boman, M. Tribological properties of highly oriented Ti(C,N) deposited by chemical vapor deposition. *Tribol. Int.* **2018**, *119*, 593–599. [CrossRef]
31. Zin, V.; Montagner, F.; Deambrosis, S.M.; Mortalò, C.; Litti, L.; Meneghetti, M.; Miorin, E. Mechanical and Tribological Properties of Ta-N and Ta-Al-N Coatings Deposited by Reactive High Power Impulse Magnetron Sputtering. *Materials* **2022**, *15*, 3354. [CrossRef]

32. Bednarik, M.; Mizera, A.; Manas, M.; Navratil, M.; Huba, J.; Achbergerova, E.; Stoklasek, P. Influence of the β^- Radiation/Cold Atmospheric-Pressure Plasma Surface Modification on the Adhesive Bonding of Polyolefins. *Materials* **2021**, *14*, 76. [CrossRef]
33. Manas, D.; Bednarik, M.; Mizera, A.; Manas, M.; Ovsik, M.; Stoklasek, P. Effect of Beta Radiation on the Quality of the Bonded Joint for Difficult to Bond Polyolefins. *Polymers* **2019**, *11*, 1863. [CrossRef]
34. Jin, H.; Lu, Y.; Ma, P.-P.; Wu, S.-S.; Shen, J. Structure and properties of irradiated HDPE high-density polyethylene/calcium carbonate composites. *J. Thermoplast. Compos. Mater.* **2014**, *29*, 893–903. [CrossRef]
35. Hu, P.; Zhao, P.-P.; Zhang, G.-W.; Wang, X.-H. Thermal properties of 60Co irradiated crosslinked high density polyethylene. *Sol. Energy Mater. Sol. Cells* **2016**, *149*, 55–59. [CrossRef]
36. Khouqeer, G.A.; Farah, K.; Toumi, S.; Hosni, F. Electron paramagnetic resonance characterization of gamma and electron irradiated high-density polyethylene: Possible use as a high-dose dosimeter. *Nucl. Eng. Technol.* **2025**, *57*, 103419. [CrossRef]
37. Bezprozvannych, G.V.; Pushkar, I.A. Influence of gamma radiation on the electrical and mechanical properties of on-board systems cables. *Eletr. Eng. Electromechanics* **2026**, *1*, 76–85. [CrossRef]
38. Xu, W.; Lu, K.; Li, H.; Xiong, C.; Liu, Y.; Liu, B. Electron Beam-Irradiated Cross-Linked Polyethylene Composites Containing Graphene Nanoplatelets for Thermally Conducting Pipes. *C—J. Carbon Res.* **2025**, *11*, 31. [CrossRef]
39. Khonakdar, H.A.; Jafari, S.H.; Wagenknecht, U.; Jehnichen, D. Effect of electron-irradiation on cross-link density and crystalline structure of low- and high-density polyethylene. *Radiat. Phys. Chem.* **2006**, *75*, 78–86. [CrossRef]
40. Chen, C.J.; Boose, D.C.; Yeh, G.S.Y. Radiation-induced crosslinking: II. Effect on the crystalline and amorphous densities of polyethylene. *Colloid Polym. Sci.* **1991**, *269*, 469–476. [CrossRef]
41. Lee, J.H.; Jeong, H.Y.; Lee, S.Y.; Cho, S.O. Effects of Electron Beam Irradiation on Mechanical and Thermal Shrinkage Properties of Boehmite/HDPE Nanocomposite Film. *Nanomaterials* **2021**, *11*, 777. [CrossRef] [PubMed]